

THE FINE STRUCTURE OF
ACANTHAMOEBA CASTELLANII
(NEFF STRAIN)

II. Encystment

BLAIR BOWERS and EDWARD D. KORN

From the National Heart Institute, Laboratory of Biochemistry, the Section on Cellular Physiology, National Institutes of Health, Public Health Service, U. S. Department of Health, Education, and Welfare, Bethesda, Maryland 20014

SUMMARY

Encysting cells of *Acanthamoeba castellanii*, Neff strain, have been examined with the electron microscope. The wall structure and cytoplasmic changes during encystment are described. The cyst wall is composed of two major layers: a laminar, fibrous exocyst with a variable amount of matrix material, and an endocyst of fine fibrils in a granular matrix. The two layers are normally separated by a space except where they form opercula in the center of ostioles (exits for excysting amebae). An additional amorphous layer is probably present between the wall and the protoplast in the mature cyst. Early in encystment the Golgi complex is enlarged and contains a densely staining material that appears to contribute to wall formation. Vacuoles containing cytoplasmic debris (autolysosomes) are present in encysting cells and the contents of some of the vacuoles are deposited in the developing cyst wall. Lamellate bodies develop in the mitochondria and appear in the cytoplasm. Several changes are associated with the mitochondrial intracristate granule. The nucleus releases small buds into the cytoplasm, and the nucleolus decreases to less than half its original volume. The cytoplasm increases in electron density and its volume is reduced by about 80%. The water expulsion vesicle is the only cellular compartment without dense content in the mature cyst. The volume fractions of lipid droplets, Golgi complex, mitochondria, digestive vacuoles, and autolysosomes have been determined at different stages of encystment by stereological analysis of electron micrographs. By chemical analyses, dry weight, protein, phospholipid, and glycogen are lower and neutral lipid is higher in the mature cyst than in the trophozoite.

INTRODUCTION

Populations of the small soil amoeba, *Acanthamoeba castellanii*, can be induced to encyst under laboratory conditions (17). Induction is apparently linked to the extrinsic cues of increase in osmotic pressure and decrease in carbon sources. Successful encystment requires oxygen and the presence of calcium or magnesium ions (2, 17). The initiation of encystment in these amoebae induces a redirec-

tion of metabolism so that a previously naked cell synthesizes a chemically and structurally complex cell wall. Wall synthesis is accompanied by a decrease in cytoplasmic mass and a gradual dehydration of the organism. The resulting cyst is a viable cell that can withstand prolonged starvation, desiccation, cold, and heat (1, 17).

The encystment of *Acanthamoeba* is a differentia-

tion uncomplicated by sexual processes, and, as already emphasized by Neff (17), provides a useful system for the study of cellular morphogenesis. Some of the interrelated processes leading to the production of an encysted organism can be followed by morphological studies. The cell organelles which contribute to the cellular remodeling can be identified and, to some extent, the contribution that each organelle makes to the end result can be inferred.

The fine structure of the trophozoite of *Acanthamoeba* has been described in a previous paper (6). The present study describes the structure of the cyst wall and the cytoplasmic changes that occur during the encystment. Cytoplasmic changes that can be correlated with encystment are most evident in the mitochondria, the Golgi complex, and the digestive vacuole system. Other more subtle changes can be observed in the nucleus, the water expulsion vesicle (contractile vacuole), and in the cytoplasmic reserves. Changes in concentration of protein, lipid, and glycogen occur and have been measured chemically. Vickerman (24, 25) and Bauer (4) have also described some of the fine structural changes during encystment in *Acanthamoeba*.

MATERIALS AND METHODS

The organism, the procedures for routine culture, and methods of fixation for electron microscopy have been described previously (6). Encystment was induced by the following procedure described by Neff et al. (17). Cells from agitated cultures, 7 days after subculture, were collected aseptically and incubated at 30° in an aerated salt solution of the composition: 0.1 M KCl, 0.008 M MgSO₄, 0.0004 M CaCl₂, and 0.02 M 2-amino-2-methyl-1,3-propanediol. The initial pH varied between 7.4 and 7.8. 5 hr after transfer to encystment medium, the pH was adjusted to 9.0 with 1 M NaOH. The rate of initiation of encystment was followed by cell counts with results similar to those obtained by Neff et al. (17). After 16 hr in encystment medium, 99% of the cells had initiated encystment. Samples of cells for electron microscopy were taken at 1 or 2 hr intervals between 0 and 18 hr and at 24 and 46 hr. Cells were also taken from stationary cultures that had encysted slowly over a period of several weeks in growth medium, as well as from continually agitated cultures which were also allowed to encyst spontaneously.

Measurements

The average diameter of ameboid cells was determined as follows: an agitated 7 day culture was har-

vested by low-speed centrifugation and the cells were resuspended in 4×10^{-4} M 2,4-dinitrophenol in 0.1 M sodium phosphate buffer, pH 6.8. The cells were centrifuged after 5–10 min and were fixed immediately in 3% glutaraldehyde in the same buffer. The cells appeared uniformly round after this treatment and showed no extended pseudopods. The diameters of 1000 cells were measured with an eyepiece micrometer and a 40 × objective. To test whether fixation caused a change in volume, the diameters of 100 unfixed cells, suspended in the same medium, were measured. The average diameters of the two groups were not significantly different. The cytoplasmic diameters of 420 unfixed, mature cysts from stationary cultures that were allowed to encyst completely were also measured.

Nuclear and nucleolar diameters of 50 ameboid and encysted cells were measured on 1 μ sections of cells fixed and embedded for electron microscopy. Nuclear diameters were measured only if a nucleolus was also present in the section.

Quantitation of Electron Micrographs

Volume fractions of lipid droplets, digestive vacuoles, autolysosomes, mitochondria, and the Golgi complex were determined at several stages of encystment from micrographs by using the Delesse principle and a regular point lattice as described by Weibel, Kistler, and Scherle (27). 13–16 micrographs which showed a section of the entire cell were used for each point shown in Fig. 12. Since a few cells at all stages of encystment were present at all times, the micrographs analyzed for each point were selected to be in comparable stages of wall formation. In the case of the 8 hr sample, some micrographs actually came from earlier or later samples but all showed the degree of wall formation that predominates in 8 hr samples. Additional details are given in the legend to Fig. 12.

Acid Phosphatase

Cytochemical tests for acid phosphatase were performed on cells that had been in encystment medium for 8 hr. The cells were fixed in cold, redistilled 3% glutaraldehyde in 0.1 M cacodylate buffer, pH 7.2, washed in the same buffer with 0.15 M KCl, and incubated in the Gomori medium as modified by Barka and Anderson (3) for 10 min at 37°. Controls were incubated at 37° for 20 min in the same medium, either with the addition of 0.01 M NaF or without substrate. After incubation the cells were rinsed briefly in cold 1% acetic acid, post-osmicated, and embedded in Epon. The results were confirmed at the light microscope level with the naphthol AS-TR phosphate-hexazonium pararosanilin method described by Barka and Anderson (3).

Chemical Analyses

The cell densities of suspensions of trophozoites and cysts were determined by direct count and by measurement of the optical density at $660\text{ m}\mu$ (28). Other aliquots of the cell suspensions were analyzed for protein by the method of Lowry et al. (12). The

remainder of the cells was extracted with 20 vol of chloroform-methanol, 2:1, and the lipid-free residue was washed with acetone and ether, then dried to constant weight. Samples of the residue were analyzed for protein to confirm the previous analysis. The rest of the residue was extracted with 30%

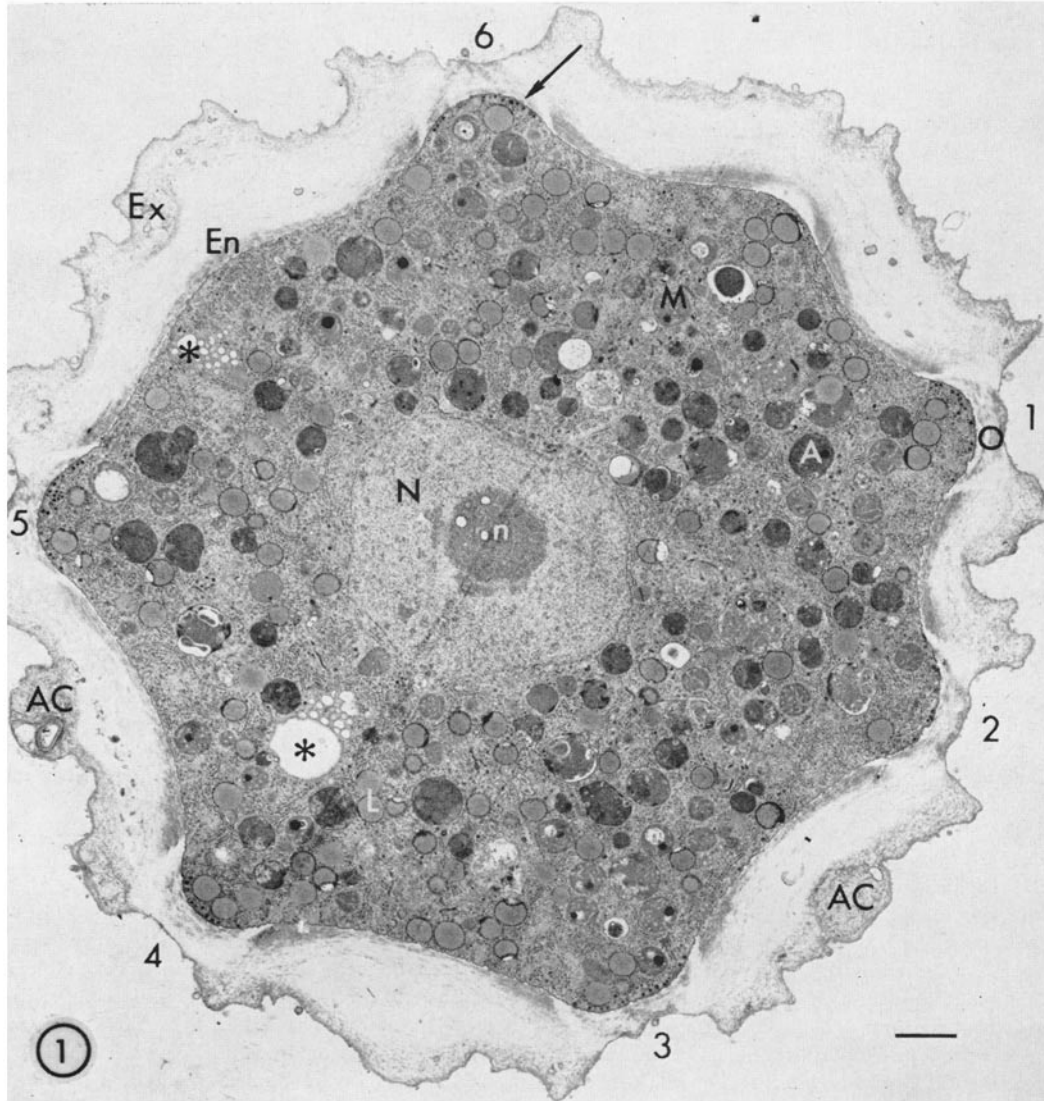


FIGURE 1 Cross section of an encysting amoeba after 15 hr in encystment medium. The dense cytoplasm is packed with lipid droplets (*L*), spherical mitochondria (*M*) and autolysosomes (*A*). The cytoplasm forms bulges at each ostiole (numbered 1-6) and there is an accumulation of Golgi vesicles (arrow) at the plasma membrane in this region. The cyst wall consists of two layers, an exocyst (*Ex*) and an endocyst (*En*) which form a specialized operculum (*O*) over the ostioles. Cell debris (*AC*) deriving from autolysosomes is present in the wall. *N*, nucleus; *n*, nucleolus; asterisk, water expulsion vesicle. $\times 7620$.¹

¹ Scale lines on figures are 1μ , except where otherwise indicated.

KOH for 3 hr at 90° to extract glycogen. The polysaccharide was precipitated from the extract by addition of ethanol to a final concentration of 65%. The precipitate was dissolved in water and reprecipitated several times. The glycogen content was measured by the anthrone reaction (22). The lipid extract was evaporated to dryness, dissolved in chloroform, and separated into neutral lipids (chloroform-eluate) and phospholipids (methanol-eluate) by column chromatography on silicic acid. Glycerides were determined in the neutral lipid fraction by ester assay according to Rapport and Alonzo (20). Phospholipids were analyzed by both ester and phosphorus determinations (7). The values in microequivalents were converted to micrograms, assuming molecular weights of 900 and 850 for the glycerides and phospholipids, respectively.

OBSERVATIONS

Wall Structure

The mature cyst wall consists of an outer layer (exocyst) and an inner layer (endocyst) separated

by a space (Fig. 1). A variable number of differentiated regions (ostioles) occur in which a central compact structure (operculum) is encircled by a space that is free of fibrous wall material. An excysting ameba exists through the ostiole after displacement of the operculum (18, 26). The ultrastructures of the exocyst, endocyst, ostiole, and operculum are described in the following sections.

EXOCYST

The exocyst comprises several morphologically distinct components of which the sequence of deposition can be determined by examination of cells taken at different times from a culture undergoing induced encystment. The wall component first detectable in encysting cells is an amorphous, discontinuous layer about 10 μ thick just outside the plasma membrane (Fig. 2). This material appears before the cell rounds up completely. By the time sufficient material accumulates to form a layer covering the entire surface (Fig. 2, inset), the

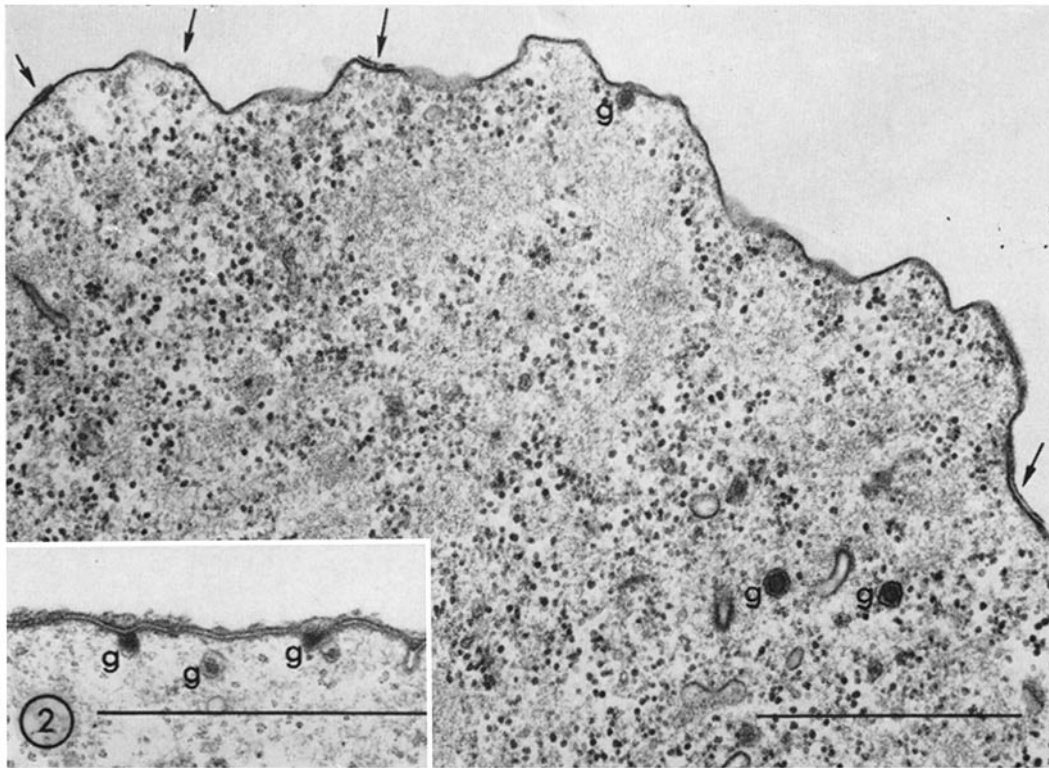


FIGURE 2 Edge of an ameba showing the earliest signs of wall synthesis. Golgi vesicles (at *g*) appear to release their content at the surface (arrows). $\times 34,000$. *Inset*: slightly later stage in wall synthesis. $\times 42,500$.

cell has become nearly spherical. In the mature cyst the underlying exocyst appears to be organized in layers parallel to the cell surface (Fig. 3). In tangential section each layer resembles a fibrillar network with interspersed, ill-defined amorphous substance (Fig. 4). In cells induced to encyst in salt solution, the exocyst is often of loose texture and without distinct layering (Figs. 1, 6) as compared with cells that have encysted in growth medium (Figs. 3, 5). The exocyst in both cases terminates in a very loose fibrous layer (Figs. 1, 3). The entire exocyst is 0.3–0.5 μ thick.

Material recognizable as cytoplasmic debris is often stuck to the outer surface of the exocyst, trapped in pockets between the exocyst layers (Figs. 1, 4, 6), or, less frequently, is scattered throughout the wall. The occasional misleading impression that the cyst wall is bounded by an external trilaminar membrane (Fig. 5) is apparently due to the tendency of components of his debris to spread over the surface of the cyst.

Particles are often seen within the exocyst (Figs. 4, 9) that resemble the intracellular glycogen granules both in the morphological state and in the presence of granular deposits after staining with lead (Fig. 7).

ENDOCYST

The endocyst differs from the exocyst in texture and in staining characteristics. Its fibrous nature is difficult to resolve with the electron microscope; it often appears to be finely granular (Fig. 4). However, at high magnification fibrils can sometimes be seen as negative images embedded in a granular matrix (Fig. 3). The fibrils of both the exocyst and the endocyst appear to be less than 50 Å in diameter.

The endocyst is consistently separated from the exocyst by a zone of the same electron density as that of the embedding plastic. This region does not react with stains for light microscopy. Only a

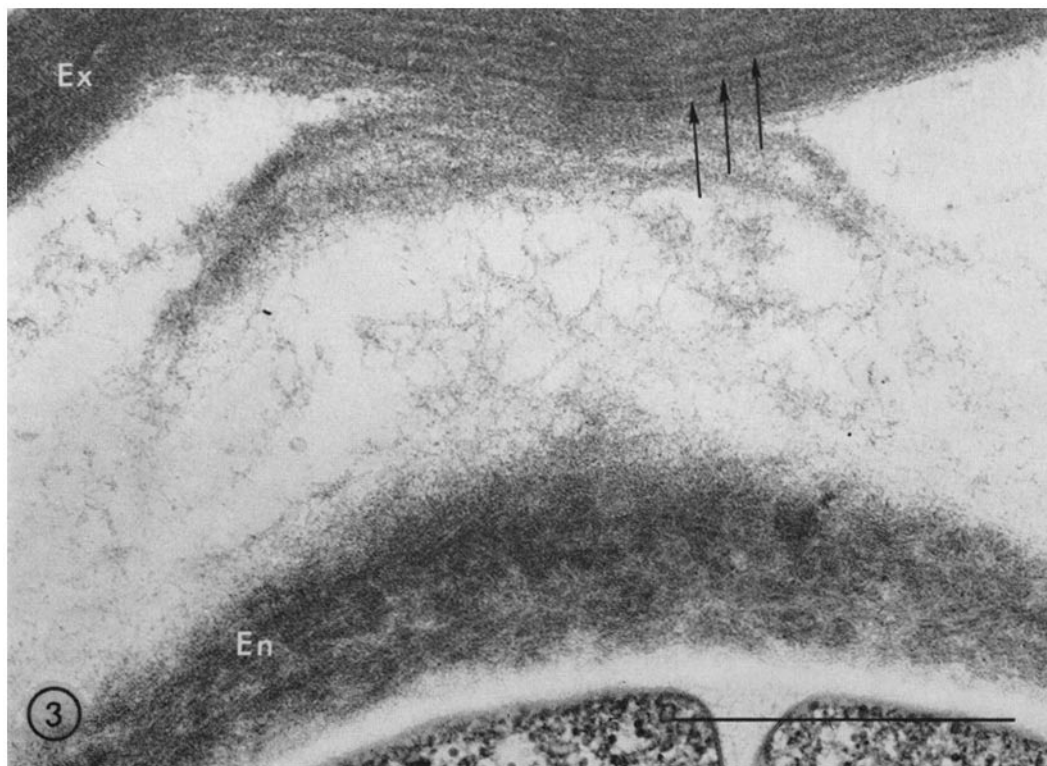


FIGURE 3 Cross section of a wall of a cell that encysted spontaneously in growth medium. The exocyst (*Ex*) shows distinct layering (arrows), and the endocyst (*En*) shows unstained fibrils embedded in a dense matrix. $\times 44,600$.

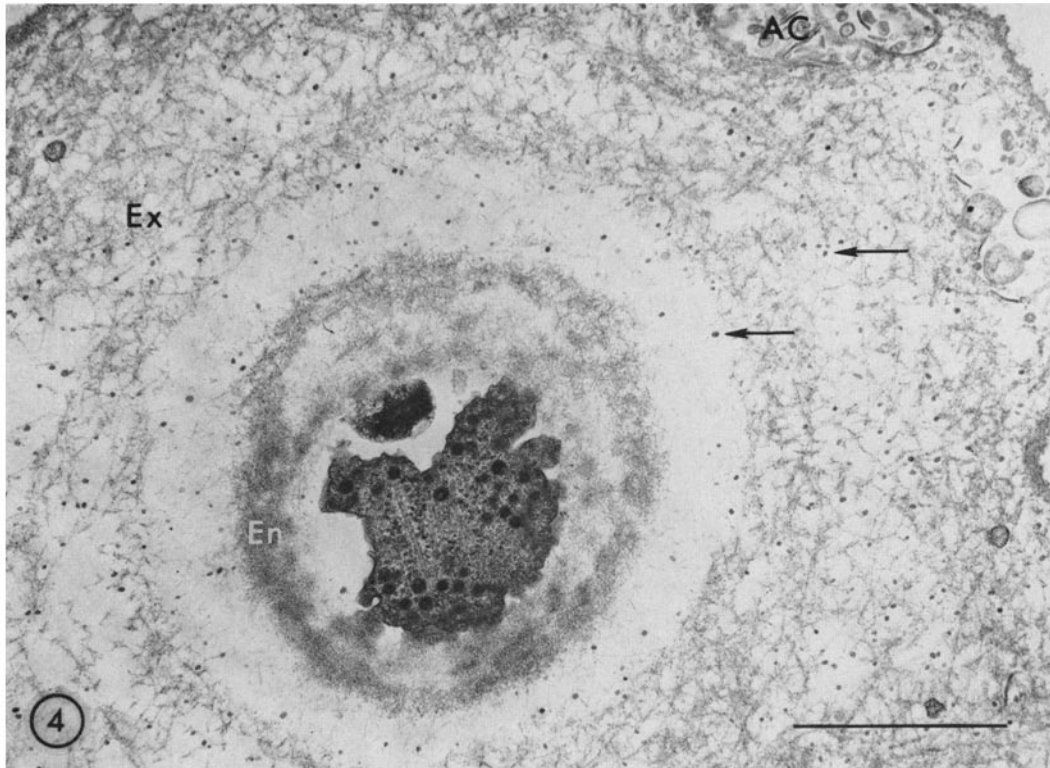


FIGURE 4 Tangential section through an ostiole region of a cyst wall. The fibrous nature of the exocyst (*Ex*) is easily seen, while the endocyst (*En*) appears granular. Note the glycogen particles (arrow) scattered throughout wall (see Fig. 7 for identification) and cell debris (*AC*) embedded in pockets in the wall. The cytoplasm under the ostiole contains many Golgi vesicles and several microtubules. This cyst wall contains less electron-dense material than the cyst walls shown in Figs. 3 and 5, resembling more closely the cyst walls of the cells shown in Figs. 1 and 6. $\times 27,200$.

few scattered fibrils can be observed within it in the electron microscope (Figs. 1, 3, 8).

There is no consistent or well-defined space between the plasma membrane and the endocyst as the latter is being deposited; but in the mature cyst there is a space of about 0.1μ between the inner wall and the plasma membrane (Figs. 8, 9). This zone is less electron dense than the plastic-embedding matrix and, thus, it very likely represents an additional amorphous layer.

OSTIOLES

The outermost layer ($30\text{--}50 \text{ m}\mu$ thick) of the exocyst is continuous over the entire surface of the cell (Fig. 5). At periodic intervals, however, the underlying exocyst and endocyst (which elsewhere are separated) are closely apposed and terminate, thus delimiting an annular space that contains neither exocyst nor endocyst (Figs. 4, 5). The cen-

ter of the ostiole is occupied by the operculum, a segment of closely apposed exocyst and endocyst (Fig. 5). The exocyst is thinner in the operculum than elsewhere in the wall whereas the endocyst is generally thicker in both the operculum and the regions immediately around it than in the rest of the wall (Fig. 1).

Cytoplasmic Changes

The mean diameter of rounded ameoboid cells was found to be $26.5 \pm 0.17 \mu$ whereas the mean cytoplasmic diameter of cysts was $16.2 \pm 0.13 \mu$. The decrease in surface area during encystment of a cell of median diameter was calculated to be more than 65%. The decrease in median cell volume was about 80%. The large decrease in cell surface implies a significant loss of cell membrane but the only morphological clues to possible mechanisms are the long infoldings of surface

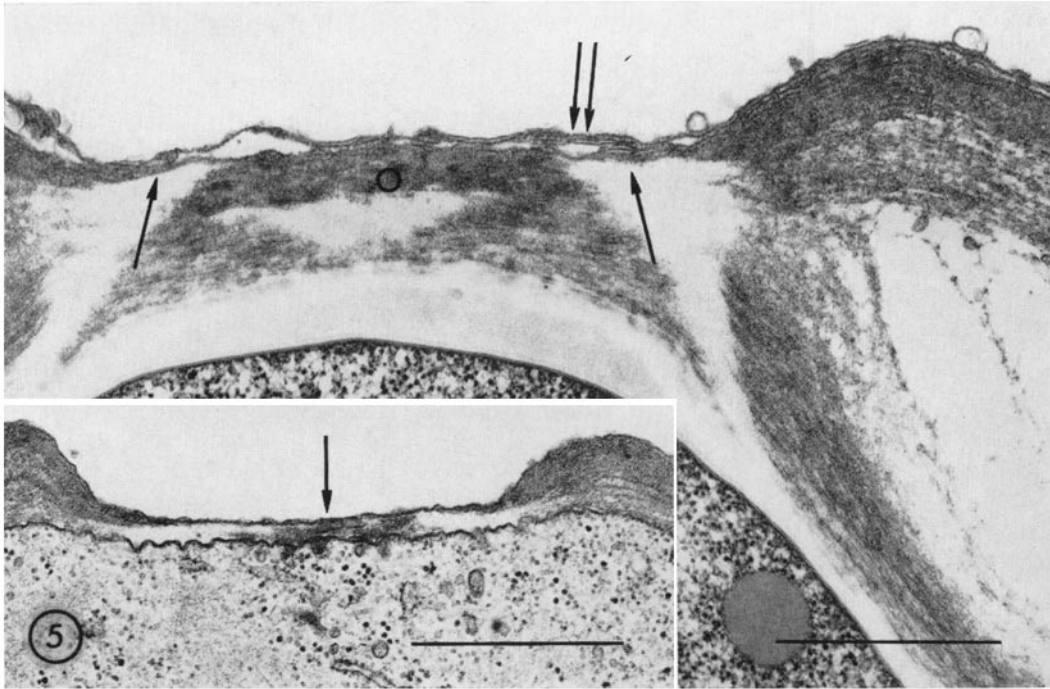


FIGURE 5 Cross section of a cyst wall in the region of the ostiole. The operculum (*O*) is composed of two layers that are structurally similar to the exo- and endocyst. Note the presence of trilaminar structures on the outer layer of the exocyst (double arrows) and the continuity of the outermost layer (single arrows) of the exocyst across the ostiole. $\times 28,900$. *Inset*: This cell has a complete layer of exocyst, but no endocyst. The outer layer of the operculum (arrow) is being laid down in the center of a circular area covered only by the outermost layer of the exocyst. $\times 27,000$.

membrane that occur early in encystment (Fig. 10). The extremely dense cytoplasm of encysted cells in both light and electron micrographs suggests that the volume change is partially the result of dehydration. Specific cytoplasmic alterations that accompany encystment are described in the following sections. By relating the cytoplasmic changes to the appearance of the cell wall, it is possible to determine the stage of encystment at which these changes occur and occasionally to suggest possible interrelationships.

GOLGI COMPLEX

Both the form and the distribution of the Golgi complex change during encystment. The Golgi complex of the trophozoite quite often occurs as large aggregates of cisternal stacks (see Fig. 7 in reference 6); however, the Golgi complex of encysting cells is more widely distributed in smaller aggregates (Fig. 6). The volume fraction of the Golgi complex in encysting cells increases about

sixfold early in encystment and thereafter returns to its original volume fraction of about 0.5% (Fig. 12).

The earliest morphological changes detected in encysting cells are the concurrent appearances of the thin, incomplete layer of amorphous material outside the plasma membrane (Fig. 2) and the densely staining material within the Golgi complex (Fig. 11). Many small vesicles about 70μ in diameter appear to bud off the Golgi cisternae. Similar vesicles, labeled by their dense content, are also seen at the cell surface (Fig. 2) where they appear to release their content (Fig. 2, inset). The densely staining content of the Golgi complex gradually diminishes at the time the endocyst is being formed and is usually absent in mature cysts.

AUTOLYSOSOMES

Large basophilic granules are a prominent component of the cytoplasm of encysting amebae

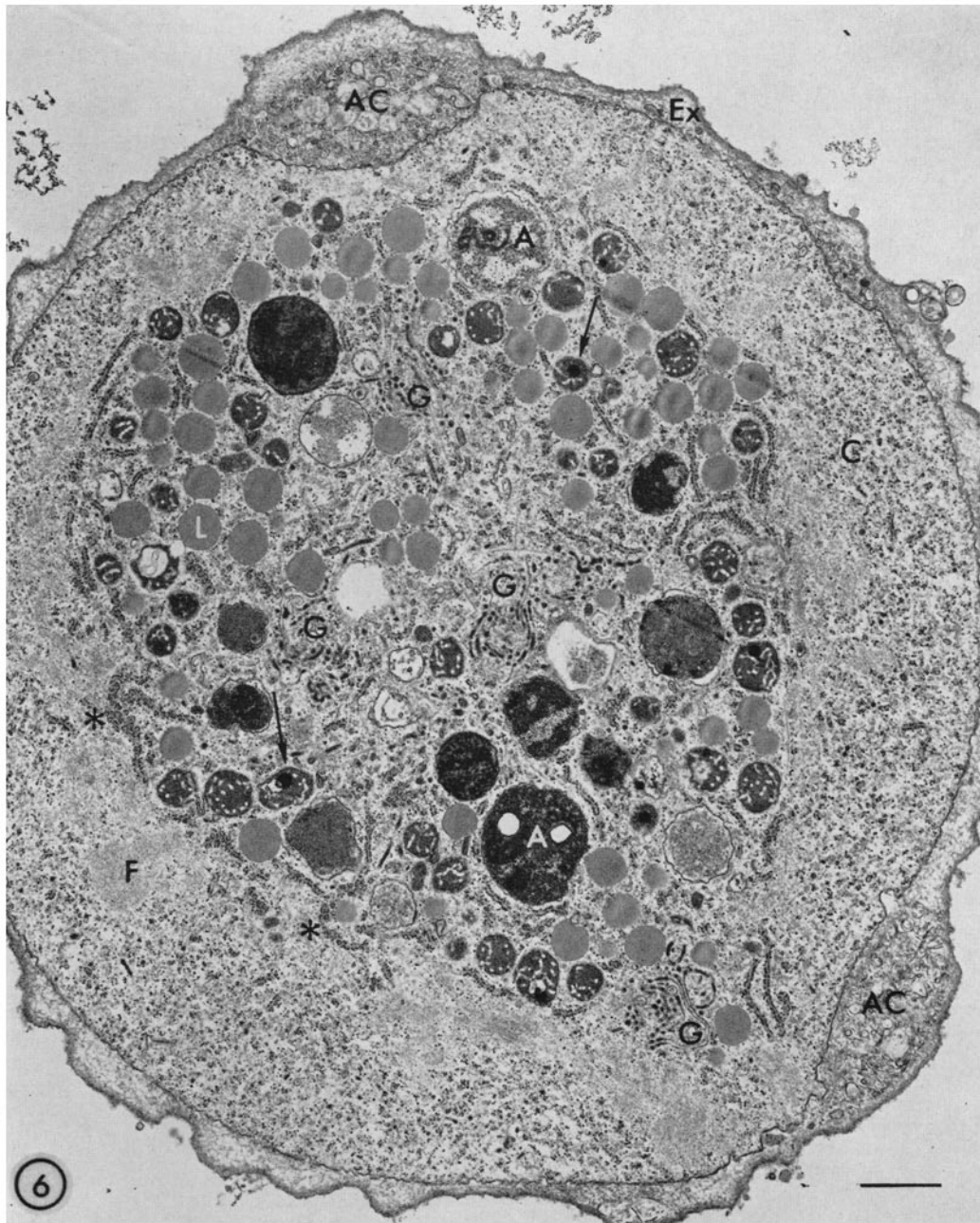


FIGURE 6 Cross section of an ameba in which exocyst (*Ex*) synthesis is nearing completion. A cortex (*C*) of hyaline cytoplasm is present and contains patches of fibrous material (*F*). Several Golgi complexes (*G*) are present. Some mitochondria show lamellate bodies lying nearby and a dense intracristate droplet (arrows). Note also the circular patterns of ribosomes on tangentially sectioned endoplasmic reticulum (asterisks). *A*, autolysosomes; *L*, lipid; *AC*, extruded cell debris. $\times 10,500$.

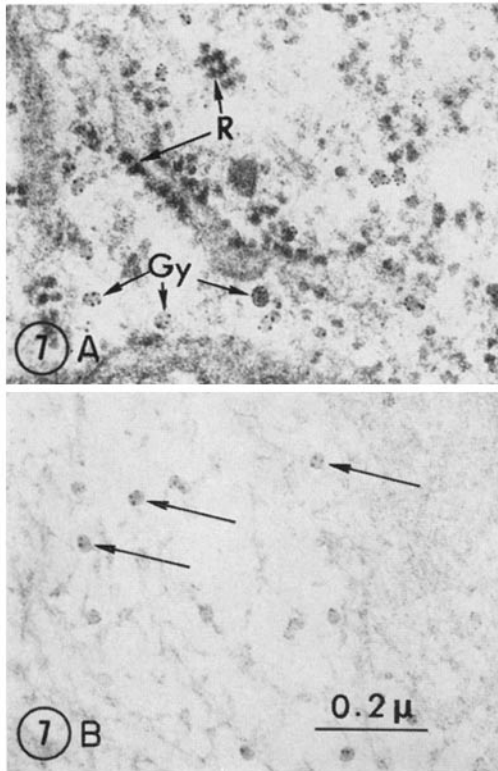


FIGURE 7 Unique staining reaction of glycogen particles. Fig. 7A is a portion of cytoplasm showing ribosomes (*R*) and glycogen particles (*Gy*) with a granular appearance. The granular stain enables us to identify particles in the exocyst (7B and Figs. 4 and 9) as glycogen (arrows). $\times 72,800$.

when viewed through the light microscope (18, 21). These granules can be readily identified by use of the electron microscope as vacuoles with dense content that includes mitochondria, lipid droplets, and glycogen (Figs. 6, 10, 11). By cytochemical methods, the vacuoles can be shown to contain acid phosphatase (Fig. 13 and ref. 4). The positive staining reaction for acid phosphatase and the recognizable cytoplasmic components are the criteria which define these vacuoles as autolysosomes (8).

Autolysosomes appear very early in encystment and are present in the cytoplasm by the time the exocyst forms a complete layer around the cell. The images in Fig. 14 A and B of areas of cytoplasm segregated by a space which is limited by a single dense line, presumably represent early stages in the formation of autolysosomes. The membrane limit-

ing the segregating space does not show trilaminar structure at the magnifications used in this study. This is in contrast to the membrane surrounding the autolysosome (Fig. 14) which has an asymmetric trilaminar image similar to that of the digestive vacuole and the plasma membrane (6).

The volume fraction of autolysosomes increases for 18 hr during induced encystment and many autolysosomes are still present in mature cysts (Fig. 12). In dehydrated, mature cysts cytoplasmic components cannot be identified within the autolysosomes and crystalline structures are present (Fig. 9).

MITOCHONDRIA

Coiled lamellate structures appear within the mitochondria after cells have been in encystment medium for 1-2 hr (Fig. 15 A, B, and D). These structures appear to arise by compaction and by coiling of tubular entities. They lie in an enlarged space between cristae, often adjacent to the intracristate granule. The lamellate structures usually, but not invariably, appear to be extruded from the mitochondria. Many such structures are seen apparently free in the cytoplasm (Figs. 6 and 15 A). Mitochondria in cells in later stages of encystment no longer show the lamellate bodies. The lamellate structures are probably related to starvation rather than to encystment per se because they are also seen in the mitochondria of cells that have remained amoeboid after many hours in encystment medium.

In encysting cells a very electron-dense concretion develops in the center of the small amorphous granule present in the intracristate space of mitochondria of trophozoites (4, 6, 24). This concretion, usually less than 0.1μ in diameter, is completely electron opaque (Fig. 15 F). Frequently the embedding medium fails to penetrate the concretion so that it drops out of the section. These characteristics suggest that it is inorganic material. By the time the exocyst is complete, many mitochondria have also developed a large spherical droplet, lying adjacent to, or surrounding the granule and its concretion (Fig. 15 C and F). The droplets may approach 0.3μ in diameter. In more dehydrated cysts, the droplet is seen to bulge out of the mitochondrion often in a multipartite fashion (Fig. 15 E and G) and is surrounded by a trilaminar membrane. The droplet appears in some cases to have become detached from the mitochondrion.

The mitochondria of the dehydrated cyst still

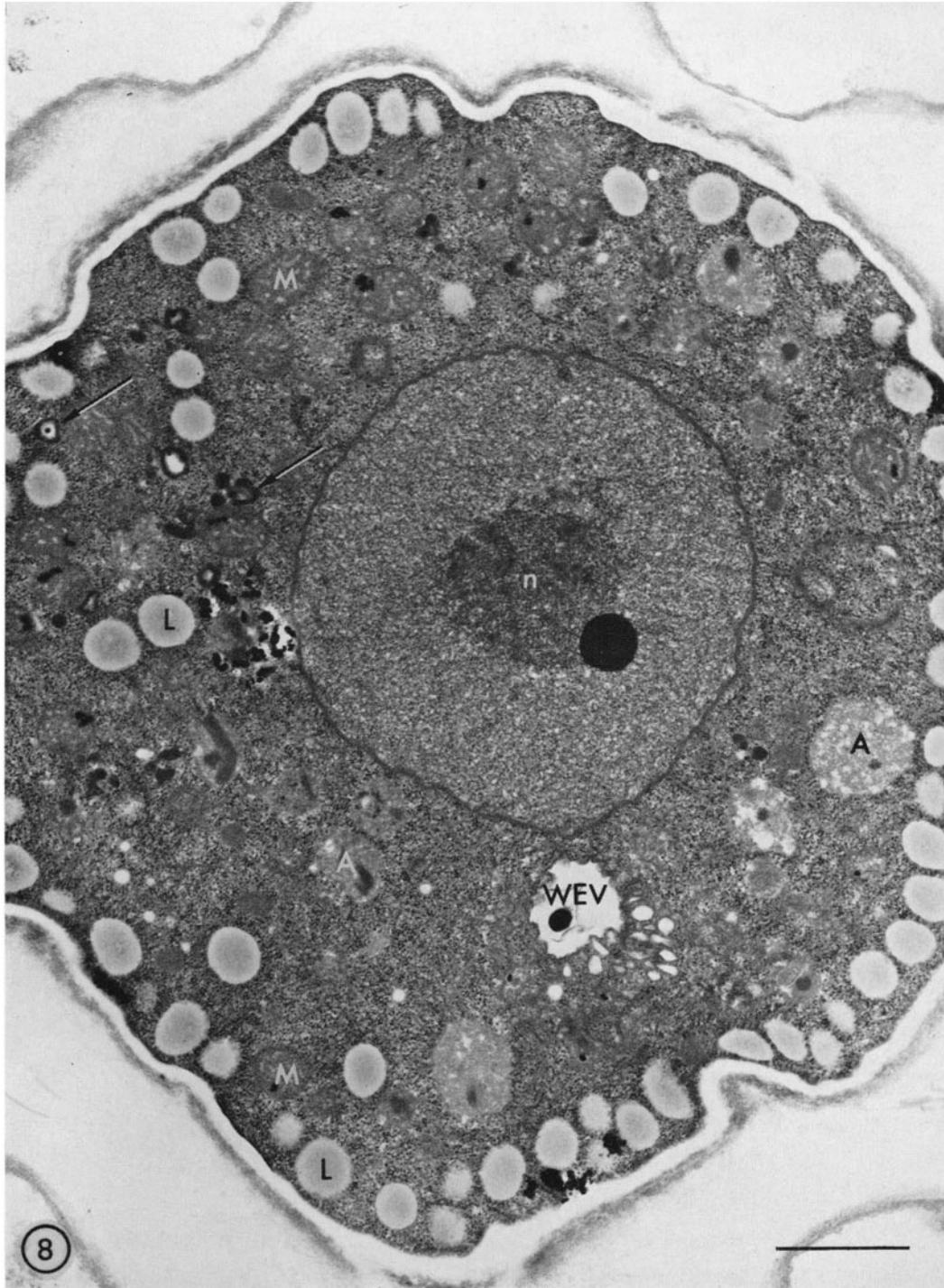


FIGURE 8 An encysted amoeba after 46 hr in encystment medium. A nucleolus (*n*) with a dense droplet is present in the nucleus. Lipid droplets (*L*) have assumed a peripheral position just under the plasma membrane. The water expulsion vesicle (*WEV*) and its associated structures are the only compartment that remains free of dense content. *A*, autolysosomes; *M*, mitochondria; arrows, droplets extruded from mitochondria. (See Fig. 15). $\times 18,600$.

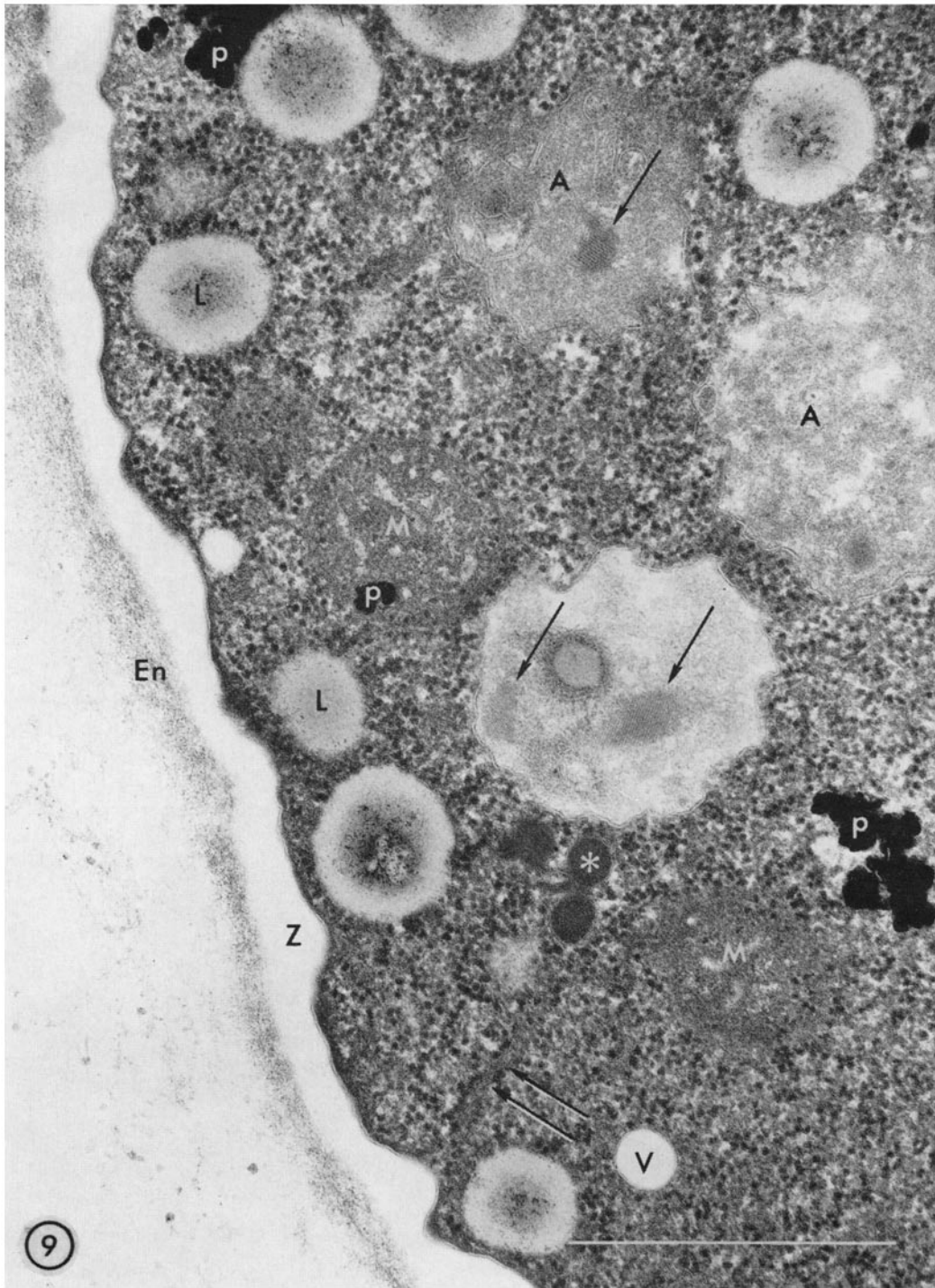


FIGURE 9 Edge of an encysted cell after 46 hr in encystment medium. An amorphous zone (*Z*) separates the protoplast from the endocyst (*En*). Mitochondria (*M*) are barely visible against the dense cytoplasm. Crystalline material (arrows) is present in the autolysosomes (*A*). Note the membrane-bounded dense material that apparently derives from a mitochondrion (asterisk). Evidence for the mitochondrial origin of this material is presented in Fig. 15. The dense precipitates (*p*) that look like surface contamination are within the section and occur randomly throughout the cytoplasm in some encysted amoebae. Similar deposits have been observed in other amoebae (See ref. 29) and their origin is unknown. *L*, lipid; double arrow, rough endoplasmic reticulum; *V*, vesicle belonging to the water expulsion system. $\times 47,100$.

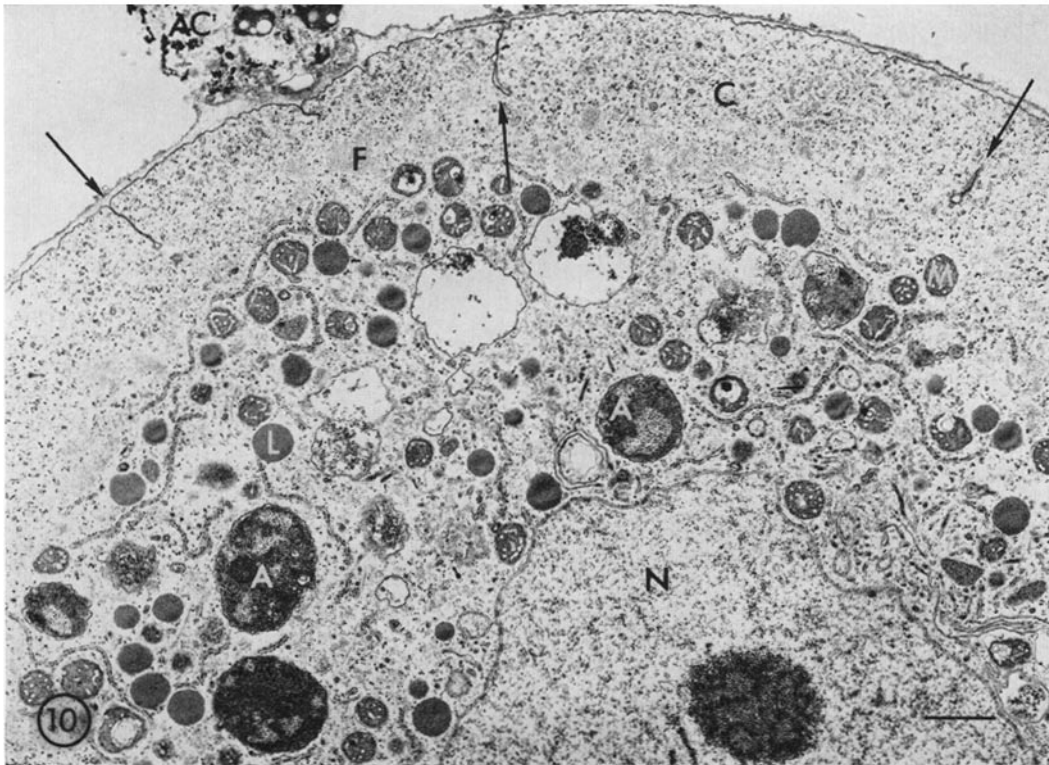


FIGURE 10 Section of an ameba in the early stages of exocyst secretion after 8 hr in encystment medium. Larger formed elements of the cell are excluded from a cortex (*C*) which occupies most of the cell periphery. The cortex includes fibrillar material (at *F*). Note also the long infoldings of plasma membrane (arrows). *A*, autolysosomes; *L*, lipid, *M*, mitochondria; *AC*, extruded cell debris; *N*, nucleus. $\times 8700$.

contain tubular cristae, but they are poorly defined relative to those in the trophozoite and are only about $34\text{ m}\mu$ in diameter (Figs. 9, 15), compared to about $60\text{ m}\mu$ in the trophozoite. The mitochondrial matrix is very dense, and ribosome-like granules are still present. Paracrystalline and filamentous structures (which are present in the mitochondria of ameboid cells [6]) cannot be seen, if indeed they are present, in these dense mitochondria. The mitochondria are incorporated into autolysosomes (Figs. 6, 10, 14) but they remain a fairly constant fraction of the cell cytoplasm throughout encystment (Fig. 12).

OTHER ORGANELLES

The endoplasmic reticulum (*ER*) of encysting cells is predominantly cisternal in form. Ribosomal clusters in circular or spiral array are prominent on

tangential sections of the cisternae (Figs. 6, 16). The densely staining content of the *ER* that is often present in the trophozoite (6) has not been observed in the *ER* of encysting cells; nor have patches of smooth *ER* been seen which are found in the trophozoite (6).

A cortex resembling the hyaline cytoplasm (ectoplasm) of the ameboid cell is often present at the periphery of the cell (Figs. 6, 10, 16) during deposition of the exocyst. Lipid droplets, mitochondria, and autolysosomes are largely absent from the cortex, but small segments of rough *ER* may be present. The fibrous material that is found in the pseudopods of the ameboid cell is primarily found in the cortex during exocyst formation, at which time it appears to encircle the central region of the cell (Figs. 6, 10, 16). By the time endocyst formation begins there is no longer a pronounced

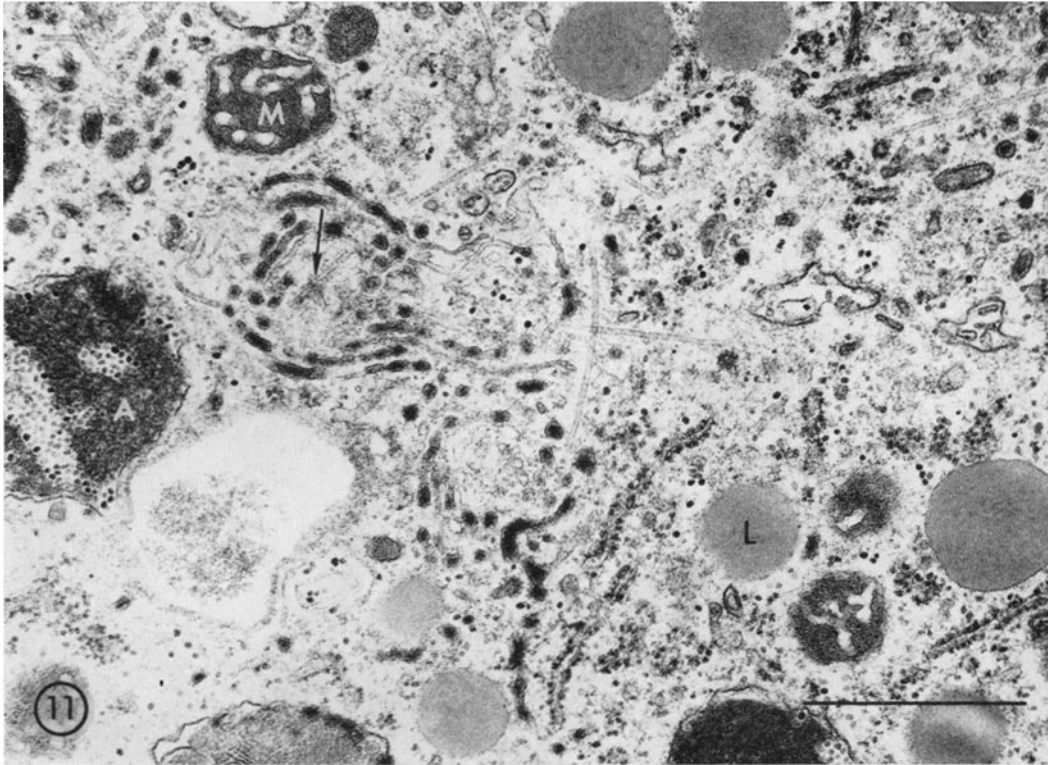


FIGURE 11 Golgi complex of the amoeba shown in Fig. 6. The Golgi cisternae contain a densely staining material which appears to be released by vesiculation of the cisternae. Note the focus of microtubules in the center of the Golgi complex (arrow). *A*, autolysosome; *M*, mitochondrion; *L*, lipid. $\times 28,900$.

cortex and the fibrous material is still visible after wall synthesis is complete, but it cannot be discerned in the dense, mature cyst.

Cytoplasmic microtubules can be seen at all stages of encystment. During exocyst deposition the microtubules seem to be confined to the central region of the cell except under the ostioles where they are near the plasma membrane (Fig. 4). Later, during endocyst deposition, microtubules are found in all regions of the cell. The microtubules of encysting cells often show the same focal relationship with the Golgi complex (Fig. 11) that is found in the trophozoite (6).

The digestive vacuole system which is characterized in the axenically cultured trophozoite by the presence of a light, flocculent precipitate within the vacuoles (6), disappears as a recognizable component during encystment (Fig. 12).

The water expulsion vesicle (*WEV*) remains free of any dense content throughout encystment. The *WEV*, often partially collapsed, and its associated

small vesicles stand out in bold relief against the dense cytoplasm of the dehydrated cyst (Figs. 1, 8, 9). We have not observed a tubular spongione in encysted cells similar to that found in the amoeboid cell (6, 25).

In early encystment, the nucleus becomes lobulated forming small nuclear buds (Fig. 16) which do not appear to contain nucleolar material. Many of the nuclear buds are incorporated into autolysosomes (Fig. 14 B). The mean nuclear diameter of the trophozoite was $6.3 \pm 0.21 \mu$ and that of the mature cyst was $5.6 \pm 0.24 \mu$. Because of the difficulty in measuring a true nuclear diameter in 1μ sections, these values may be an underestimate but they do suggest a decrease in nuclear volume of at least 40% during encystment.

The measured mean diameters of the nucleoli of trophozoites and cysts were $2.4 \pm 0.08 \mu$ and $1.5 \pm 0.07 \mu$ respectively, which suggests a reduction in nucleolar volume of about 75%. Part of the densely staining material of the nucleolus ap-

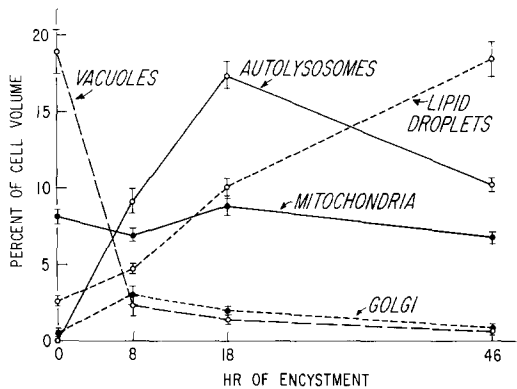


FIGURE 12. Volume fraction of cell elements at several stages of encystment. The data were obtained by differential point counts on electron micrographs. The brackets are individually 90% confidence intervals for the true volume fractions of each cell element. The values at zero hour were obtained from ameoboid cells from 7 day agitated cultures. The values for encysting cells were obtained from several experiments in which encystment was induced. At 8 hr cells have synthesized only the exocyst; by 18 hr cells have synthesized both the exocyst and endocyst; and by 46 hr cells have a complete cyst wall and dense cytoplasm. Autolysosomes are defined as vacuoles that contained cytoplasmic debris. Vacuoles include both digestive vacuoles and the water expulsion vesicle, but not autolysosomes. The only vacuoles present at 18 and 46 hr are the water expulsion vesicles. The stereological data are internally consistent and accurately reflect changes that occur during encystment, but they may not be a true indication of the absolute percent volume of each element in the whole cell.

appears to disperse in the nucleoplasm during encystment. Its subsequent fate is difficult to determine morphologically. In the mature cyst the nucleolus develops a large, dense droplet (Fig. 8). The droplet is most commonly found in cysts which have been in encystment medium more than 24 hrs, but it is also found in cysts from agitated cultures in growth medium. Whether droplet formation is a normal part of encystment is not known.

CYTOPLASMIC RESERVES

The concentration of neutral lipid increases during encystment (Table I). There is a concomitant decrease in phospholipid (Table I), therefore total lipid remains relatively constant. The volume fraction of lipid droplets increases from 2.6% in ameoboid cells to 18% in 46 hr-encysted cells (Fig. 12). This increase in partial volume is due

both to an increase in absolute amount of neutral lipid and to a decrease in the volume of other cell components as a result of dehydration.

The glycogen content of cysts is very much less than that of trophozoites (Table I). Glycogen granules appear to comprise an appreciable proportion of the content of the autolysosomes in early encystment (Fig. 11).

DISCUSSION

Several investigators have described encystment in living *Acanthamoeba* as observed by phase-contrast microscopy. These observations are valuable in providing a framework into which fit the more detailed, but necessarily discontinuous, observations made with the aid of the electron microscope.

The first morphological signal of encystment is the rounding of the cell (17, 18, 21, 25, 26). At this early stage no wall is visible when employing the light microscope, but use of the electron microscope reveals a thin layer of exocyst. Considering the concurrent appearance of dense material in the Golgi complex and in its associated vesicles, and the presence of similar vesicles at the cell surface, which are apparently releasing their content, it seems most probable that this outermost amorphous layer of the exocyst is secreted via the Golgi complex. With these morphological studies, it is difficult to document the possible involvement of the Golgi complex in the synthesis of the rest of the exocyst and especially of the endocyst (when the dense content of the Golgi complex is diminished)

As the ameoboid cell becomes spherical, numerous cytoplasmic "granules" appear in the cytoplasm (18, 21, 25). Using the electron microscope we identified these bodies as autolysosomes on the basis of their content and positive staining reaction for acid phosphatase. The appearance of autolysosomes in encysting ameobae correlates with the disappearance of "empty" digestive vacuoles (Fig. 12), suggesting that segregated portions of the cytoplasm, such as those seen in Fig. 14 A and B, may in some way be incorporated into digestive vacuoles. The present observations elucidate neither the source of the hydrolytic enzyme(s) in the autolysosomes, nor the origin of the membrane segregating the cytoplasm.

The contents of food vacuoles (in bacteria-fed ameobae) are discharged during encystment (21, 25). The present study and that by Bauer (4), of axenically cultured ameobae, show clumps of

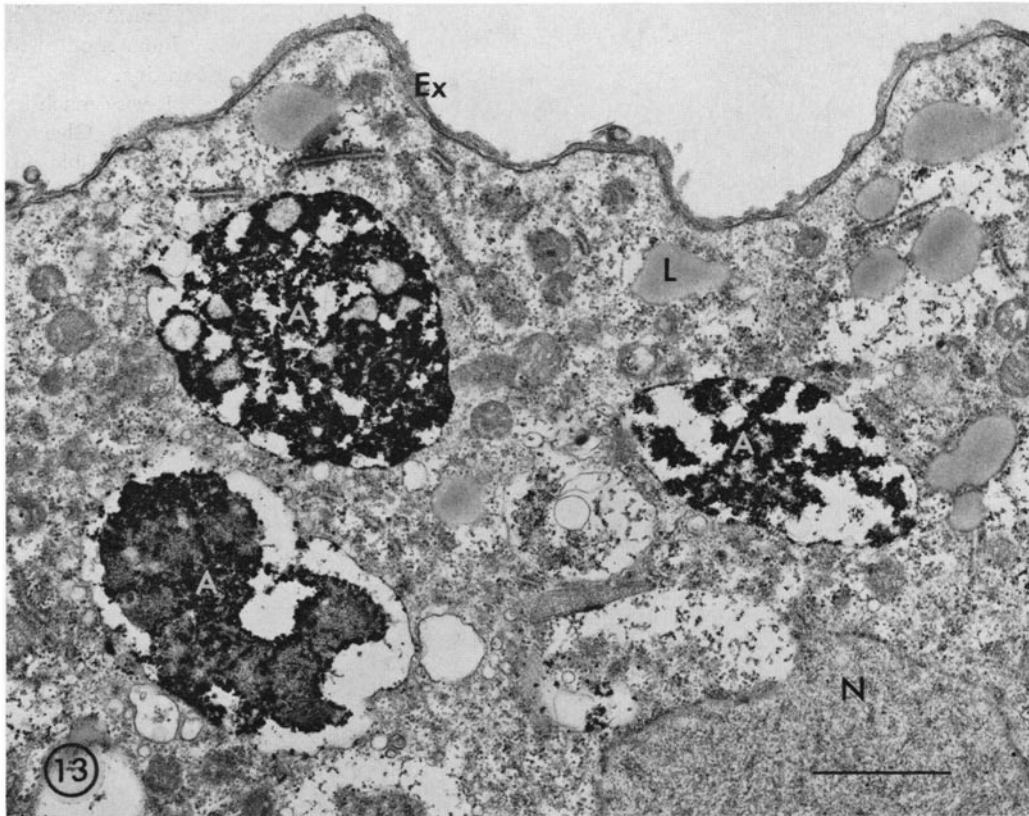


FIGURE 13 An amoeba at an early stage in exocyst synthesis that has been incubated for 10 min in Gomori medium to demonstrate acid phosphatase. Membrane-bounded vacuoles (*A*) that correspond to vacuoles containing cytoplasmic debris (autolysosomes) show a positive reaction. Cells incubated in the presence of NaF or without substrate do not show the dense vacuolar precipitate. *N*, nucleus; *L*, lipid; *Ex*, exocyst. $\times 18,200$.

cytoplasmic debris trapped in the cyst wall and images that suggest discharge of autolysosomal content into the wall. In this study the clumps of cell debris were found predominantly in the exocyst, so that autolysosomes, which are present in the mature cyst, appear to be much less frequently discharged after endocyst formation begins.

Autolysis and excretion of cytoplasmic constituents are consistent with the decrease in dry weight, protein, phospholipid, and glycogen which we have measured (Table I). The appearance of soluble proteins, amino acids, and ribonucleotides in the medium of encysting cultures has also been reported (10). Although it is reasonable to suppose that some of the autolysed material is used as a source of precursors for cell wall synthesis or as a

source of energy for the cell that has no external food source, morphological studies cannot provide evidence for such metabolic events.

The details of mitochondrial changes during encystment are visible only in the electron microscope. Vickerman (24) has described the change in shape of the mitochondria and the increase in size of the intracristate granule. Coiled, lamellate structures also appear in the mitochondria. The lamellate structures, which seem to derive from compacted tubular elements, do not appear to be fixation artifacts because they are not present in growing cells fixed in an identical manner. They do occur in the occasional cell that remains amoeboid in encystment medium. Similar structures have been observed in other protozoa during starvation (11); therefore, it is likely that

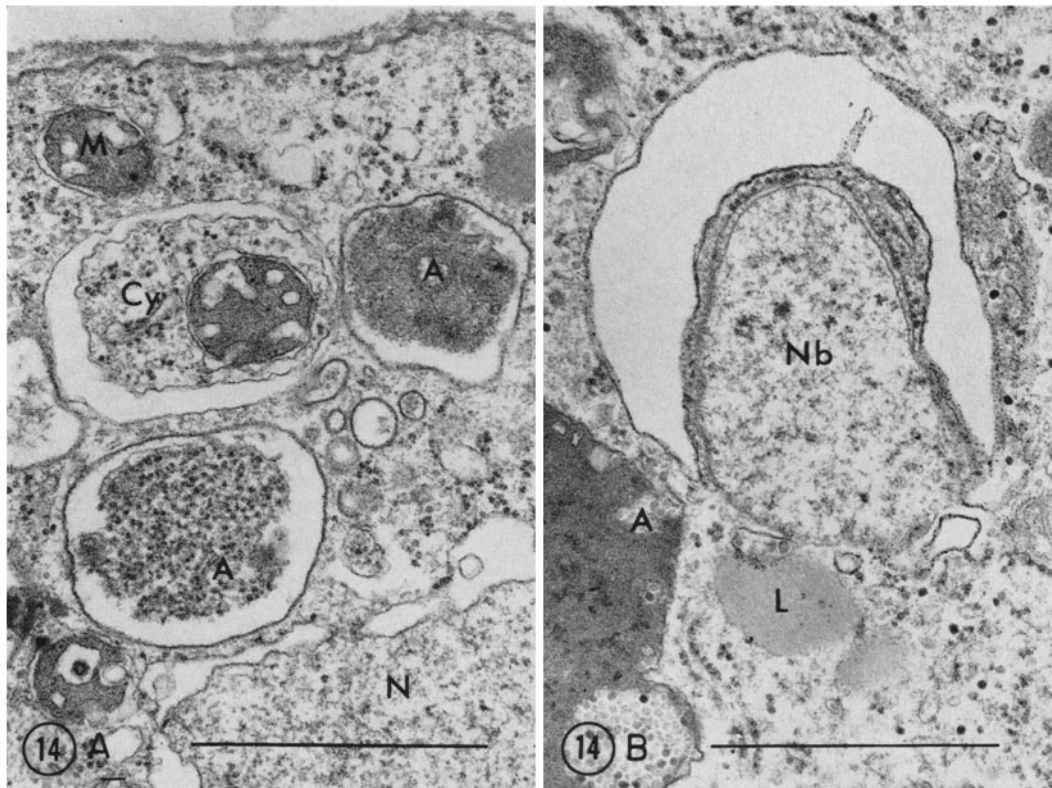


FIGURE 14 Possible origin of autolysosomes in the cytoplasm of an encysting amoeba. Fig. 14A, a cisterna limited by a single dense line appears to be segregating a small area of cytoplasm (*Cy*). Two small vacuoles (*A*) contain dense material within a single, trilaminar limiting membrane. *N*, nucleus; *M*, mitochondrion. Fig. 14B, a region similar to that shown in Fig. 14A that shows a nuclear bud (*Nb*) in the segregated portion of cytoplasm. *A*, autolysosome; *L*, lipid. $\times 37,800$.

TABLE I
Chemical Analysis of Trophozoite and Encysted Cells

	Trophozoite	Cyst
	$\mu\text{g}/10^6$ cells	
Lipid free dry weight	706	397 (56)*
Protein	489	276 (57)
Glycogen	83	18 (22)
Glycerides	56	67 (120)
Phospholipid	59	47 (80)

Results are from one induced encystment experiment. Trophozoites were from pooled agitated cultures, 6 and 7 days after subculture. Cysts were taken for analysis after the cells were in encystment medium for 21 hr at which time they were 99.6% encysted.

* Figures in parentheses give the per cent of the corresponding value for trophozoites.

their formation during encystment is related to starvation. A decrease in respiration of whole cells and of isolated mitochondria during encystment has been reported (9). This may be related to the development of the various droplets and dense granules in mitochondria. The mitochondrion of the mature cyst appears to retain essentially the same structure as the mitochondrion of the trophozoite but to be much condensed.

Some hours after the beginning of wall synthesis, the protoplast retracts from the wall (21, 25). An increased rate of discharge of the water expulsion vesicle occurs at about the same time (21), which suggests that the retraction of the protoplast is mainly the result of dehydration (1, 21, 25). The protoplast remains close to the outer wall in the regions of the ostioles (18, 21, 26 and Fig. 1) forming conical projections, or "mammillae"

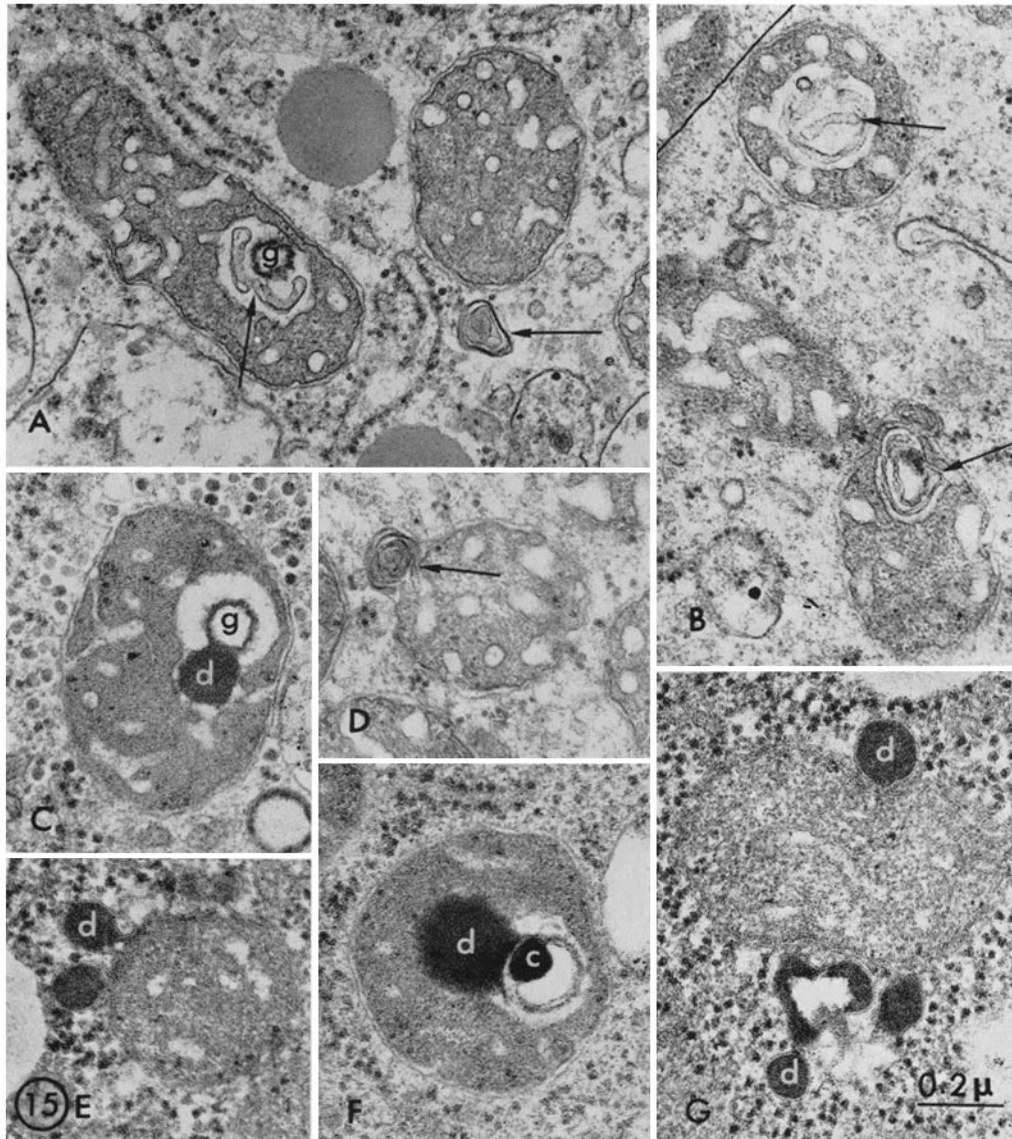


FIGURE 15 Early mitochondrial changes in encysting cells that are also present in starving cells are shown in Fig. 15A, B and D. There appears to be an accumulation of tubular material in the intracristate space, which is compacted and extruded as a lamellate structure (arrows). Figs. 15C and 15F show the droplet (*d*) which forms adjacent to the granule in later stages of encystment. Fig. 15F also shows a dense concretion (*c*) that frequently develops in the center of the mitochondrial granule (*g*). Figs. 15E and 15G show mitochondria from mature cysts in which it appears that the droplet has been extruded from the mitochondrion and is surrounded by a distinct trilaminar membrane. $\times 55,100$.

(13). Bundles of microtubules are frequently seen in the mammillae (shown tangentially in Fig. 4) and may contribute to the maintenance of these projections (19). A possible clue to the time of dehydration relative to wall formation is suggested by the fact that the endocyst follows closely the shape of the plasma membrane and not that of the exocyst. It may be that the space between

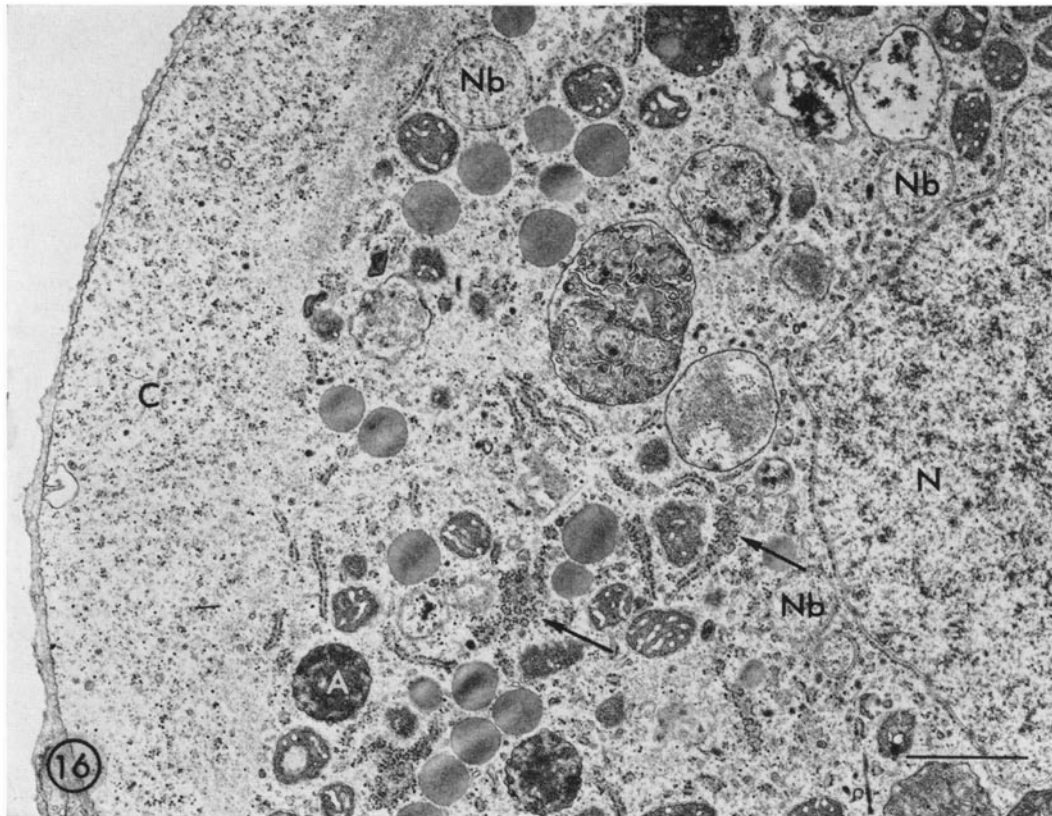


FIGURE 16 An encysting amoeba in the early stages of exocyst synthesis showing nuclear budding (*Nb*). Note also the prominent cortex of hyaline ectoplasm (*C*) and the patterned arrays of ribosomes (arrows). *N*, nucleus; *A*, autolysosome. $\times 15,200$.

the exocyst and endocyst results from cellular dehydration after completion of the exocyst but before the formation of the endocyst. We have occasionally observed cells in which the exocyst and endocyst were complete and of normal appearance except that the two layers were tightly apposed and very smooth. In these cases the cytoplasm showed no increase in density as compared to the cytoplasm of the trophozoite and had apparently failed to dehydrate normally.

The chemical composition of the cyst wall in *Acanthamoeba* has not been precisely defined. Tomlinson and Jones (23) have identified cellulose in isolated cyst walls. Neff and Benton (14) reported the localization of cellulose in the endocyst by cytochemical means, and Page (18) has confirmed the strong reaction of the endocyst to the cytochemical test for cellulose. Neff, Benton, and Neff (15) also report the presence of substantial

amounts of protein in the isolated wall. Bauer (4) has identified hydroxyproline in the cyst wall and finds the major incorporation of radioactive hydroxyproline to be in the exocyst, suggesting that the latter contains a peptide or protein component. The electron microscope images do not further elucidate the chemical composition but they do emphasize the structural differences between the wall layers. On this basis, it seems very likely that the two wall layers are also chemically different. The large amount of cytoplasmic debris that may be entrapped in the cyst wall must be allowed for in the interpretation of chemical analyses.

The distribution and organization of hyaline cytoplasm may be important in both the sequence of deposition of wall layers and in the differential deposition of wall material that results in the formation of ostioles. In the careful studies of Ray and Hayes (21), variations in streaming rates and

the appearance and disappearance of hyaline ectoplasm during the synthesis of cell wall were observed. The absence of ectoplasm under the ostioles was also noted. The electron micrographs are consistent with these observations and commonly show a pronounced cortex during exocyst production except under regions of potential ostioles. The electron micrographs also show a concentration of microtubules and an accumulation of vesicles with electron-dense content under the ostioles (Fig. 1). The microtubules, in conjunction with the fibrous material, may be involved in directed cytoplasmic movements (19) that affect the differential synthesis of exocyst and endocyst in the operculum.

From observations on sectioned material, Volkonsky (26) has described the partial expulsion of peripheral chromatin during encystment. This observation seems to be corroborated by our observation of nuclear budding, and may be related to the data of Neff and Neff (16) that suggest that encystment occurs after cellular arrest in the DNA synthetic phase. The decrease

in nucleolar size noted in this study has also been observed previously in both fixed (26) and living (21) cells.

Finally, it should be mentioned that, at least under laboratory conditions, many cells do not encyst normally. Cysts with multiple layers of endocyst, and cysts within cysts occur, especially in cultures that have been allowed to encyst in growth medium. In induced encystment, cells with disorganized cytoplasm are present at all stages of wall formation and the complete walls appear to contain less material than those of cells encysting in growth medium.

A preliminary account of this work was given at the 7th Annual Meeting of the American Society for Cell Biology at Denver, Colorado, 13 November 1967 (5).

We are grateful to Mr. Thomas E. Olszewski for excellent technical assistance and to Mr. William R. Fairweather, National Heart Institute, Biometrics Research Branch, for assistance with statistics.

Received for publication 22 October 1968, and in revised form 12 January 1969.

REFERENCES

- ADAM, K. M. G. 1964. A comparative study of Hartmannellid amoebae. *J. Protozool.* **11**:423.
- BAND, R. N. 1963. Extrinsic requirements for encystation by the soil amoeba, *Hartmannella rhysodes*. *J. Protozool.* **10**:101.
- BARKA, T. and P. J. ANDERSON. 1962. Histochemical methods for acid phosphatase using hexazonium pararosanilin as coupler. *J. Histochem. Cytochem.* **10**:741.
- BAUER, H. 1967. Ultrastruktur und Zellwandbildung von *Acanthamoeba* sp. *Vierteljahresschr. Naturforsch. Ges. Zurich* **112**:173.
- BOWERS, B., and E. D. KORN. 1967. Fine structural changes during the encystment of an amoeba. *J. Cell Biol.* **35**:15A.
- BOWERS, B., and E. D. KORN. 1968. The fine structure of *Acanthamoeba castellanii*. I. The trophozoite. *J. Cell Biol.* **39**:95.
- DAVIDOFF, F., and E. D. KORN. 1963. Fatty acid and phospholipid composition of the cellular slime mold, *Dictyostelium discoideum*. *J. Biol. Chem.* **238**:3199.
- DEDUVE, C., and R. WATTIAUX. 1966. Functions of lysosomes. *Ann. Rev. Physiol.* **28**:135.
- GRIFFITHS, A. J., D. LLOYD, G. I. ROACH, and D. E. HUGHES. 1967. Metabolic changes in *Hartmannella castellanii* during encystment. *Biochem. J. (England)*. **103**:21P.
- GRIFFITHS, A. J., G. I. ROACH, and D. E. HUGHES. 1966. Early stages in the encystment of *Hartmannella castellanii*. *J. Protozool.* **13**: (suppl.) 31.
- LEVY, M. R., and A. M. ELLIOTT. 1968. Biochemical and ultrastructural changes in *Tetrahymena pyriformis* during starvation. *J. Protozool.* **15**:208.
- LOWRY, O. H., N. J. ROSEBROUGH, A. L. FARR, and R. J. RANDALL. 1951. Protein measurement with Folin phenol reagent. *J. Biol. Chem.* **193**:265.
- NEFF, R. J. 1957. Purification, axenic cultivation, and description of a soil amoeba, *Acanthamoeba* sp. *J. Protozool.* **4**:176.
- NEFF, R. J., and W. F. BENTON. 1962. Localization of cellulose in the cysts of *Acanthamoeba* sp. *J. Protozool.* **9**: Suppl., 11.
- NEFF, R. J., W. F. BENTON, and R. H. NEFF. 1964. The composition of the mature cyst wall of the soil amoeba *Acanthamoeba* sp. *J. Cell Biol.* **23**:66A.
- NEFF, R. J., and R. H. NEFF. 1966. Induction of differentiation by antibiotics, antimetabolites, and cytostatic agents. *J. Cell Biol.* **31**:80A.
- NEFF, R. J., S. A. RAY, W. F. BENTON, and M. WILBORN. 1964. Induction of synchronous encystment (differentiation) in *Acanthamoeba*

- sp. In *Methods in Cell Physiology*. D. M. Prescott, editor. Academic Press Inc., New York. 1:55.
18. PAGE, F. C. 1967. Re-definition of the genus *Acanthamoeba* with descriptions of three species. *J. Protozool.* **14**:709.
 19. PORTER, K. R. 1966. Cytoplasmic microtubules and their functions. In *Principles of Biomolecular Organization*. Ciba Foundation Symposium. Little, Brown and Co., Boston. 308.
 20. RAPPORT, M. M., and N. ALONZO. 1955. Photometric determination of fatty acid ester groups in phospholipides. *J. Biol. Chem.* **217**:193.
 21. RAY, D. L., and R. E. HAYES. 1954. *Hartmanella astronoxis*: a new species of free-living amoeba. Cytology and life cycle. *J. Morphol.* **95**:159.
 22. SCOTT, T. A., JR., and E. H. MELVIN. 1953. Determination of dextran with anthrone. *Anal. Chem.* **25**:1656.
 23. TOMLINSON, G. and E. JONES. 1962. Cellulose in the cyst wall of a soil amoeba. *Biochim. Biophys. Acta* **63**:194.
 24. VICKERMAN, K. 1960. Structural changes in mitochondria of *Acanthamoeba* at encystation. *Nature.* **188**:248.
 25. VICKERMAN, K. 1962. Patterns of cellular organization in *Limax* amoebae. An electron microscope study. *Exp. Cell Res.* **26**:497.
 26. VOLKONSKY, M. 1931. *Hartmanella castellanii* Douglas e: classification des *Hartmanelles*. *Arch. Zool. Exp. Gen.* **72**:317.
 27. WEIBEL, E. R., G. S. KISTLER, and W. F. SCHERLE. 1966. Practical stereological methods for morphometric cytology. *J. Cell Biol.* **30**:23.
 28. WEISMAN, R. A., and E. D. KORN. 1966. Uptake of fatty acids by *Acanthamoeba*. *Biochim. Biophys. Acta* **116**:229.
 29. WOHLFARTH-BOTTERMANN, K. E. 1960. Protisten-Studien X. Licht und elektronenmikroskopische Untersuchungen an der Amöbe *Hyalodiscus simplex* n. sp. *Protoplasma.* **52**:58.